International Journal Of Engineering Research And Development
e- ISSN: 2278-067X, p-ISSN: 2278-800X, www.ijerd.com
Volume 14, Issue 8 (August Ver. I 2018), PP.01-15

Noise Reduction Disturbance Observer Global Stability and Robustness Conditions Based on the Nyquist Stability Criteria

Jesús U. Liceaga-Castro[1], Irma I. Siller-Alcalá[1], Eduardo Liceaga-Castro[2]
[1]*Department of Electronic, UAM-Azc, CDMX, México*
[2]*Areronautical Department, IPN, CDMX, México*
Corresponding Author:julc@azc.uam.mx

ABSTRACT:Global and robust stability conditions of controllers based on linear noise reduction disturbance observers (NR-DOB) are presented. These fundamental properties are analyzed by applying the Nyquist stability criteria of the overall scheme. Under this framework the stability and robustness of the control scheme are clearly exposed and established. The effectivity of the control strategy here proposed is shown through a series of illustrative examples in which systems with delays, non-minimum phase zeros or un-stable poles are considered.

Date of Submission: 29-06-2020 Date of acceptance: 20-07-2020

I. INTRODUCTION

Control schemes based on the Noise Reduction Disturbance Observer (NR-DOB) may be considered an improvement of controllers based on Disturbance Observers (DOB). Similarly, the DOB control configuration was developed from the internal model control scheme (IMC). In these three control strategies the performance and specifications are defined in terms of an internal model of the controlled process. These control strategies aim at estimating and eliminating model uncertainties, perturbations, and measurement noise.

The main characteristic of the IMC is the design of feedback controllers by accommodating in a single tuning parameter specification related to performance, robustness, and output disturbance rejection. On the other hand, DOB and NR-DOB schemes are based on two parameter configurations in which the performance and the disturbance rejection specifications are set considering different parameters, defining in this manner a two-degrees of freedom (2-DOF) control framework.

In [1-7] it is shown that by tuning the performance, robustness, and disturbance attenuation specifications under a 2-DOF framework presents advantages and more flexibility in the control design process.

In the case of NR-DOB, the components of the 2-DOF configuration are a feedback controller and a sensor noise filter. The controller is designed based on theprocess model while the filter is designed to reduce the effects of sensor noise in the control system performance. In general DOB designs cannot reduce the effects of sensor noise without affecting control system performance.

There are various reports on the effectivity of NR-DOB control designs in which a unity steady state gain filter is used to eliminate sensor noise. Nevertheless, due to the lack of a clear and transparent procedure noise filter is designed empirically.

In [8] based on a state space analysis and in [9] under a polynomial approach almost global stability conditions for NR-DOB controllers are presented. Nevertheless, a clear design procedure for the noise rejection filter is not included.

More recently a review of the NR-DOB including some guidelines for the noise filter design rendering almost global stability conditions is presented in [10]. Meanwhile, a robust stability analysis limited to the DOB control configuration is presented in [11].

In references [12-14] application of DOB controllers to a set of systems are presented. Nevertheless, the results which include stability conditions are limited to the cases treated and no general conclusions can be established.

A more comprehensive analysis of stability and robustness, limited to the DOB based controllers, is presented in [15]. In this article unstable, non-minimum-phase processes and time-delay systems are considered.

Despite the progress and efforts reported in above mentioned works there is still lacking a clear and general procedure for the design of NR-DOB based controllers. As follows global stability and robustness conditions for the NR-DOB control configuration based on the Nyquist stability criteria are presented. The following results are expressed in the classical control frequency domain. Experience has proved that this framework is very well suited to the engineering context. As follows, it is also presented a clear and transparent

procedure for designing the noise rejection filter and its existence. In addition, requirements for process model to meet stability and robustness are also established.

The article is presented as follows: in Section II, a resume of the NR-DOB is presented. In Section III, based on the Nyquist stability criteria global stability and robustness conditions are defined. In Section IV, several examples based on different structural mismatches between process and model are shown. Finally, in Section V, conclusions are presented.

II. NOISE REDUCTION DISTURBANCE OBSERVER RESUME

The block diagram of the noise reduction disturbance observer (NR-DOB) control system is depicted in Fig. 1 where the shadowed section represents the actual NR-DOB. $R(s)$, $\delta(s)$, $d(s)$ and $\eta(s)$ are the reference signal, input perturbation, output perturbation and measurement noise, respectively. $C(s)$, $G(s)$, $\tilde{G}(s)$, and $F(s)$ are the feedback controller, process, process model or reference model, and a unity steady state gain low-pass filter respectively. It is also assumed that at low frequency $|\eta(j\omega)| \approx 0$. Whereas at high frequency $|\eta(j\omega)| \neq 0$. This is a normal condition when $\eta(s)$ represents sensor noise. Also, it is assumed that $|d(j\omega)| = |\delta(j\omega)| \approx 0$ at high frequency.

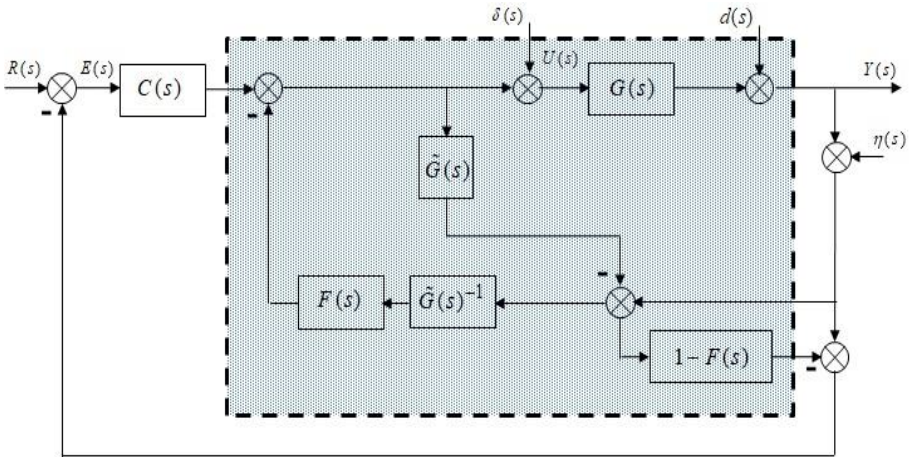

Figure 1: Noise Reduction Disturbance Observer control system

It is assumed that the filter $F(s)$ is given by:

$$F(s) = \frac{1}{(\lambda s + 1)^n} \tag{1}$$

where n is chosen such that $F(s)\tilde{G}(s)^{-1}$ is causal and $\lambda > 0$. The time constant λ of $F(s)$ is tuned mainly to determine filtering conditions for sensor the noise $\eta(s)$ and exogenous perturbations $\delta(s)$ and $d(s)$. From equation (1) is clear that filter $F(s)$ satisfy the following conditions:

$$\begin{aligned} &|F(j\omega)| \approx 1, \quad \omega \in \left[0, \omega_{B_F}\right], \\ &|F(j\omega)| \approx 0, \quad \omega \in \left[\omega_{B_F} + \Delta_\omega, \infty\right). \end{aligned} \tag{2}$$

The output of the closed-loop configuration of Fig. 1 is given by:

$$Y(s) = T_R(s)R(s) + S_d(s)d(s) + S_\delta(s)\delta(s) + S_\eta(s)\eta(s). \tag{3}$$

where:

$$T_R(s)=\frac{C(s)\,G(s)\,\tilde{G}(s)}{\left(1+\tilde{G}(s)C(s)\right)\left[\tilde{G}(s)+F(s)\left(G(s)-\tilde{G}(s)\right)\right]},$$
$$S_d(s)=\frac{\tilde{G}(s)\left(1-F(s)\right)}{\tilde{G}(s)+F(s)\left(G(s)-\tilde{G}(s)\right)},$$
$$S_\delta(s)=\frac{G(s)\tilde{G}(s)\left(1-F(s)\right)}{\tilde{G}(s)+F(s)\left(G(s)-\tilde{G}(s)\right)},$$
$$S_\eta(s)=\frac{-G(s)F(s)}{\tilde{G}(s)+F(s)\left(G(s)-\tilde{G}(s)\right)}. \tag{4}$$

Assuming denominator $\Lambda(s)=\left(1+\tilde{G}(s)C(s)\right)\left[\tilde{G}(s)+F(s)\left(G(s)-\tilde{G}(s)\right)\right]$ of equations (4) is Hurwitz and filter $F(s)$ comply with the characteristics defined by equation (1), at low frequencies, that is, at $\omega\in\left[0,\omega_{B_F}\right]$ the NR-DOB control system defined by equations (4) satisfy:

$$\left|T_R(j\omega)\right|\approx\left|\frac{C(j\omega)\tilde{G}(j\omega)}{1+C(j\omega)\tilde{G}(j\omega)}\right|,$$
$$\left|S_d(j\omega)\right|\approx 0,$$
$$\left|S_\eta(j\omega)\right|\approx -1,$$
$$\left|S_\delta(j\omega)\right|\approx 0. \tag{5}$$

On the other hand, at high frequencies, i.e. $\omega\in\left[\omega_{B_F}+\Delta_\omega,\infty\right)$, filter $F(s)$ magnitude reduces to $\left|F(j\omega)\right|\approx 0$; therefore, equations (4) can be expressed as:

$$\left|T_R(j\omega)\right|\approx\left|\frac{C(j\omega)G(j\omega)}{1+C(j\omega)\tilde{G}(j\omega)}\right|,$$
$$\left|S_d(j\omega)\right|\approx 1,$$
$$\left|S_\eta(j\omega)\right|\approx 0,$$
$$\left|S_\delta(j\omega)\right|\approx\left|G(j\omega)\right|. \tag{6}$$

From equation (6) it is clear that with a suitable filter $F(s)$ the effects of measurement noise $\eta(s)$ can be reduced without compromising tracking performance of reference signal $R(s)$. Although input and output perturbations seem to have undesired effects at high frequency, e. g. $\left|S_d(j\omega)\right|\approx 1$ and $\left|S_\delta(j\omega)\right|\approx\left|G(j\omega)\right|$. As previously mentioned, these perturbations are assumed negligible at frequencies $\omega>\omega_{B_F}$. That is, $d(j\omega)=\delta(j\omega)\approx 0$ when $\omega>\omega_{B_F}$. Therefore, the NR-DOB control strategy is an appealing option to reduce the effects of measurement noise without compromising control system performance.

III. NR-DOB STABILITY AND ROBUSTNESS CONDITIONS

The internal stability of the NR-DOB control system is defined by the following closed-loop relationships:

$$\frac{E(s)}{R(s)} = \frac{F(s)\left(G(s)-\tilde{G}(s)\right)+\tilde{G}(s)}{\left(1+\tilde{G}(s)C(s)\right)\left[\tilde{G}(s)+F(s)\left(G(s)-\tilde{G}(s)\right)\right]}, \tag{7}$$

$$\frac{E(s)}{\delta(s)} = 0, \qquad \frac{E(s)}{d(s)} = 0, \qquad \frac{E(s)}{\eta(s)} = 0,$$

$$\frac{U(s)}{R(s)} = \frac{\tilde{G}(s)C(s)}{\left(1+\tilde{G}(s)C(s)\right)\left[\tilde{G}(s)+F(s)\left(G(s)-\tilde{G}(s)\right)\right]},$$

$$\frac{U(s)}{d(s)} = \frac{U(s)}{\eta(s)} = \frac{-F(s)}{\left[\tilde{G}(s)+F(s)\left(G(s)-\tilde{G}(s)\right)\right]},$$

$$\frac{U(s)}{\delta(s)} = \frac{\tilde{G}(s)\left(1-F(s)\right)}{\left[\tilde{G}(s)+F(s)\left(G(s)-\tilde{G}(s)\right)\right]}.$$

Therefore, from equations (4) and (7) it is clear that the NR-DOB control system is globally and internally stable if polynomial $\Lambda(s) = \left(1+\tilde{G}(s)C(s)\right)\left[\tilde{G}(s)+F(s)\left(G(s)-\tilde{G}(s)\right)\right]$ is stable. This implies that:

Lemma 1: The NR-DOB control system of Figure 1 is globally and internally stable if:

i. Controller $C(s)$ stabilizes plant model $\tilde{G}(s)$. That is, polynomial $A(s) = \left(1+\tilde{G}(s)C(s)\right) = 0$ is stable.

ii. Filter $F(s)$ stabilizes polynomial:

$$B(s) = \left[\tilde{G}(s)+F(s)\left(G(s)-\tilde{G}(s)\right)\right] = 0,$$

$$B(s) = \left[1+F(s)\left(\frac{G(s)}{\tilde{G}(s)}-1\right)\right] = 0,$$

$$B(s) = \left[1+F(s)H(s)\right] = 0.$$

That is, if $F(s)$ stabilizes transfer function:

$$H(s) = \left(\frac{G(s)}{\tilde{G}(s)}-1\right) = -\left(1-\frac{G(s)}{\tilde{G}(s)}\right) = \frac{G(s)-\tilde{G}(s)}{\tilde{G}(s)}.$$

□

It is clear from *Lemma 1* that once reference model $\tilde{G}(s)$ has been selected design of controller $C(s)$ is straightforward. That is, $C(s)$ has to be designed to achieve adequate robustness and performance specifications for system $T_R(j\omega)$ defined by (5).

The design of noise filter $F(s)$ can be effectively carried out by noting that the poles of function $H(s)$ are the poles of $G(s)$ and the zeros of $\tilde{G}(s)$. Thus, the second condition of *Lemma 1* is satisfied if the Nyquist plot of $F(j\omega)H(j\omega)$ encircles N_p times anticlockwise the critical point $(-1,0)$. Where N_p is the number of right half

plane poles (RHPPs) of $G(s)$ plus the number of right half plane zeros (RHPZs) of $\tilde{G}(s)$. Further aspects need to be considered with regards to $H(s)$ zeros. It is well known that RHPZs can prevent closed-loop stabilization of any transfer function. Therefore, it is also important to determine $H(s)$ RHPZs. These can be obtained using the Nyquist stability criteria. That is, the number of RHPZs Z_H of $H(s)$ is given by:

$$Z_H = N_H + P_H$$

where:

N_H : number of clockwise encirclements to the point (1,0) of the Nyquist plot of $\tilde{G}(j\omega)^{-1}G(j\omega)$

P_H : number of RHPPs of $G(s)$ plus the number of RHPZs $\tilde{G}(s)$.

However, once model $\tilde{G}(s)$ has been designed and because filter $F(s)$ is a unity steady state gain low-pass filter, as described in equation (1), condition *ii* of *Lemma 1*reduces to design filter $F(s)$ bandwidth ω_{B_F} such that $F(s)$ does not impel the required encirclements to the point (-1,0) in anticlockwise sense of $H(s)$ or avoid, by reducing ω_{B_F}, encirclements in clockwise sense to the point (-1,0) of $H(s)$.

The former implies that if $H(s)$ is unstable with P_H unstable poles and a Nyquist plot with no P_H counter clockwise encirclements to point (-1,0), then there will not be a filter $F(s)$ capable of stabilizing polynomial $B(s)$. This infers that the stability of polynomial $B(s)$ depends mainly on the design of an appropriate internal model $\tilde{G}(s)$ such that $H(s)$ satisfies the necessary conditions for the existence of $F(s)$. This supposes that, in general, controllers based on NR-DOB are in fact 3 DOF controllers depending on: Controller $C(s)$, to satisfy performance specification, filter $F(s)$ for noise filtering properties and process model $\tilde{G}(s)$ to guarantee internal stability.

In Section IV, through different examples the design of internal model $\tilde{G}(s)$ is shown when process $G(s)$ is unstable, non-minimum phase or with time delay.

Nevertheless, if order, relative degree and steady state gain of $G(s)$ and $\tilde{G}(s)$ coincide then these systems can be written as: $G(s) = k\dfrac{b_m s^m + b_{m-1}s^{m-1} + ... + b_1 s + 1}{a_n s^n + a_{n-1}s^{s-1} + ... + a_1 s + 1}$ and $\tilde{G}(s) = k\dfrac{\tilde{b}_m s^m + \tilde{b}_{m-1}s^{m-1} + ... + \tilde{b}_1 s + 1}{\tilde{a}_n s^n + \tilde{a}_{n-1}s^{s-1} + ... + \tilde{a}_1 s + 1}$. Then, it is clear that $\lim_{\omega\to 0}\tilde{G}(j\omega)^{-1}G(j\omega) = 1$, hence $\lim_{\omega\to 0}H(j\omega) = \left(\dfrac{G(j\omega)}{\tilde{G}(j\omega)} - 1\right) = 0$. That is, $H(s)$ has a zero at the origin. At high frequency $\lim_{\omega\to\infty}\tilde{G}(j\omega)^{-1}G(j\omega) = \dfrac{b_m\tilde{a}_n}{\tilde{b}_m a_n} = M$. It is clear that if $M = 1$ then $\lim_{\omega\to\infty}H(j\omega) = \left(\dfrac{G(j\omega)}{\tilde{G}(j\omega)} - 1\right) = 0$. That is, $H(s)$ has a zero at infinity. Moreover, in the particular situation in which the corresponding parameters of the system and the model do not differ significantly it is possible to speculate that the Nyquist plot of $H(s)$ would be contained in the right-hand plane $\square_2^+$.If additionally, $\tilde{G}(s)$ and $G(s)$ are both stable and minimum phase $B(s) = \left[1 + F(s)H(s)\right] = 0$ will be stable no matter filter $F(s)$ bandwidth ω_{B_F}.

The robustness conditions of the NR-DOB control system can be defined in terms of the well-known concepts gain and phase margins. According to *Lemma 1* the requirement for robustness based on the Nyquist stability criteria are:

Lemma 2: The NR-DOB control system of Fig. 1 is robust if:

i. $C(j\omega)$ is designed such that $C(j\omega)\tilde{G}(j\omega)$ have adequate gain and phase margins
ii. $F(j\omega)$ is designed such that $F(j\omega)H(j\omega)$ have adequate gain and phase margins

□

In the ideal and unrealistic case of perfect matching between the process $G(s)$ and the process model $\tilde{G}(s)$, from equations (4) and (7), the stability and robustness conditions can be summarized as follows:

Corollary 1: When $\tilde{G}(s) = G(s)$, the NR-DOB control system will be stable and robust provided:

i. Controller $C(s)$ stabilizes the plant model $\tilde{G}(s)$ with appropriate gain and phase margins.
ii. Filter $F(s)$ is stable, and
iii. Process $G(s)$ is stable and minimum phase

Example 1: Let a stable and minimum phase process $G(s) = \dfrac{2s+10}{s^2+11s+10}$ and an unrealistic perfect model given by $\tilde{G}(s) = \dfrac{2s+10}{s^2+11s+10}$. According to *Corollary 1*, polynomial $A(s)$ must be stable so controller $C(j\omega)$ must stabilize model $\tilde{G}(s)$. A simple and suitable I controller is given by $C(s) = \dfrac{1.39}{s}$, resulting in $C(s)\tilde{G}(s)$ with phase and gain margins of $P_M = 50.6^o$ and $G_M \to \infty$, respectively. It only remains to design filter $F(s)$ whose only requirement is to be stable, as indicated by *Corollary 1*, and to assure $F(s)\tilde{G}(s)^{-1}$ causal. Therefore, from equation (1) an appropriate filter is given by $F(s) = \dfrac{1}{(0.01s+1)^2}$.

To illustrate the stability and performance of the design responses to external signals $T_R(s)R(s)$, $S_d(s)d(s)$, $S_\delta(s)\delta(s)$ and $S_\eta(s)\eta(s)$ are shown in Figure 2 assuming, for simplicity of analysis, $R(s) = d(s) = \delta(s) = \eta(s)$ unity step signals. From these responses is clear that the NR-DOB control system is globally and internally stable.

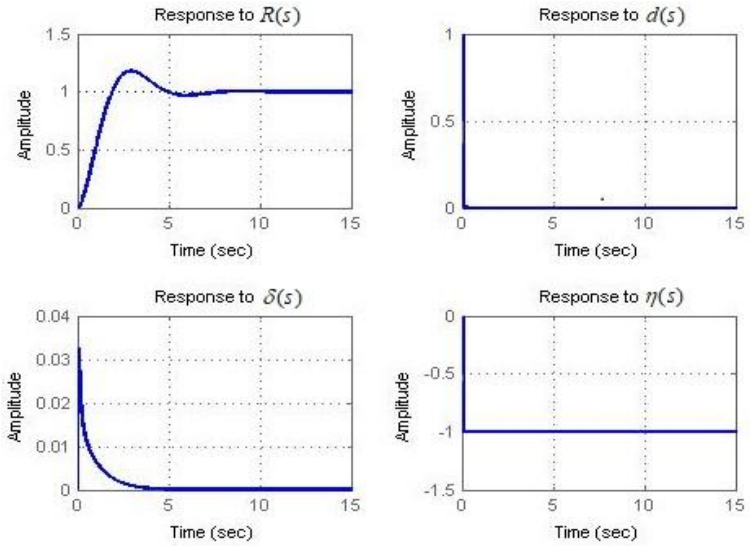

Figure 2: $T_R(s), S_d(s), S_\delta(s)$ **and** $S_\eta(s)$ **step responses.** ***Example 1***

However, the important issue arises in the realistic event of mismatch between process $G(s)$ and process model $\tilde{G}(s)$. That is, existence of filter $F(s)$ and its requirements for stability and robustness depends mainly on the mismatch between process $G(s)$ and process model $\tilde{G}(s)$. The most common mismatch between process and model is the so call sub parametrization occurring mainly when model $\tilde{G}(s)$ is simplified by neglecting high frequency modes of process $G(s)$. Although it is normally assumed that at low frequency model and process match, uncertainty in steady state gain should also be considered. Also, it is important to elucidate if NR-DOB applies to processes including time delay, non-minimum phase zeros or unstable poles.

In the following section NR-DOB control system is analysed assuming different kinds of mismatch between process $G(s)$ and model $\tilde{G}(s)$.

IV. NR-DOB CONTROL SYSTEM DESIGN EXAMPLES

As mentioned in Section III, designing NR-DOB control systems that ensure robustness, globalstability, and performance when there are mismatches between the process and the process model can become challenging. Even more so when the process is unstable, no minimum phase or with time delay. In this section, the design of NR-DOB control systems is shown, based on the classical control frequency domain analysis and *Lemmas* 1 and 2, assuming model/plant mismatch or for non-minimal phase, unstable or with time delays processes.

- *Nonminimum phase process*

Example 2: Let a stable non-minimum phase process $G(s) = 0.1\dfrac{-s+100}{s+2}$, and a sub parametrized model given by $\tilde{G}(s) = \dfrac{10}{s+2}$. Despite the differences between $G(s)$ and $\tilde{G}(s)$, in the low frequency range of $\omega \in [0, 20)\, rad/sec$, $\tilde{G}(s)$ is a good model of process $G(s)$, as shown in Figure 3.

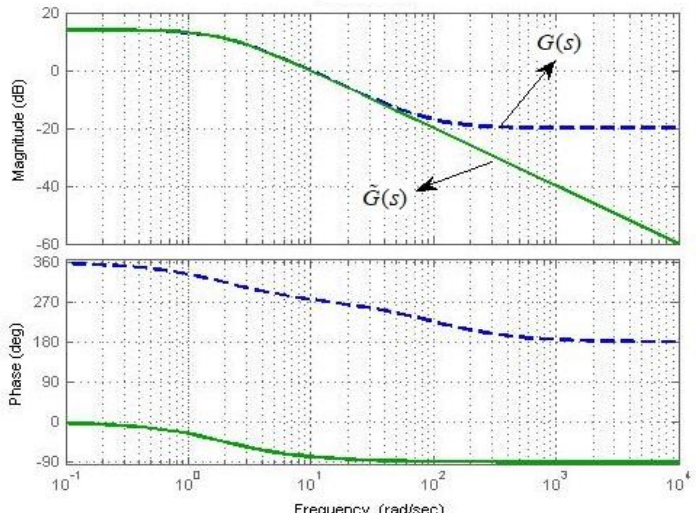

Figure 3:Bode diagrams of $G(s)$ and $\tilde{G}(s)$. *Example 2*

The first step for the design of a NR-DOB control system is, according to *Lemmas 1 and 2*, the design of a controller $C(s)$ stabilising model $\tilde{G}(s)$ with adequate phase and gain margins. A suitable PI controller is given by:

$$C(s) = \frac{(0.5s+1)}{s} \tag{8}$$

In Figure 4, the Bode diagrams of $C(s)\tilde{G}(s)$ shows adequate phase and gain margins of $P_M = 90^o$ and $G_M \to \infty$, respectively, so conditions *i* of *Lemmas 1 and 2* are satisfied.

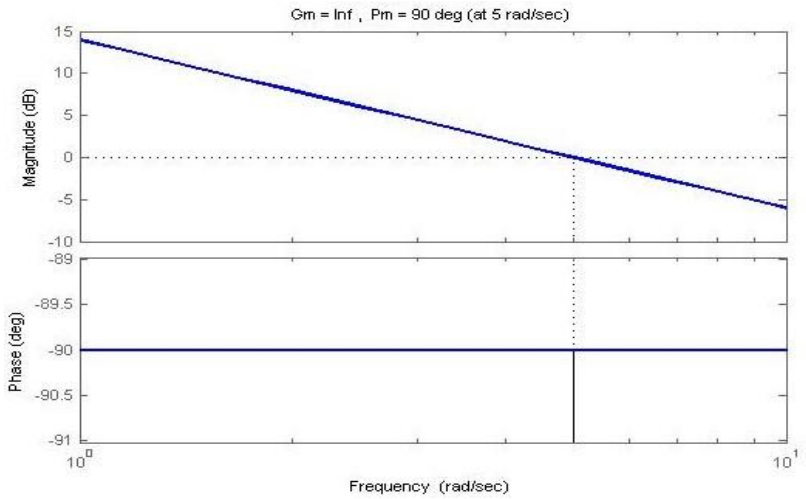

Figure 4:Bode diagrams and robustness margins of $C(s)\tilde{G}(s)$. *Example 2*

To comply with conditions*ii* of *Lemmas 1* and *2*, is necessary to calculate $\tilde{G}(s)^{-1}G(s)$ resulting in:

$$\tilde{G}(s)^{-1}G(s) = (-0.01s+1) \tag{9}$$

Since $\lim_{\omega\to 0}\tilde{G}(j\omega)^{-1}G(j\omega)=1$, $H(s)$ will have a zero at zero. In fact, $H(s)=-0.01s$ with no poles. Moreover, the Nyquist plot of $H(s)$, Figure 5, encircles the critical point (-1,0) once clockwise so an unstable pole will be induce in polynomial $B(s)$ unless filter $F(s)$ is designed with sufficiently low bandwidth ω_{B_F}, such that its roll-off avoids the clockwise encirclement to point (-1,0) of $F(s)H(s)$. This must be done also assuring appropriate robust margins and $F(s)\tilde{G}(s)^{-1}$ causal.

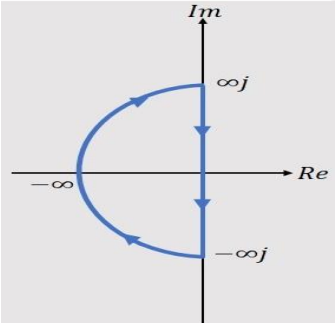

Figure 5: $H(s)$ **Nyquist plot.** ***Example 2***

A filter $F(s)$ which satisfies conditions *ii* of *Lemmas 1* and *2* is given by:

$$F(s)=\frac{1}{(0.025s+1)^2} \tag{10}$$

Bode diagrams and Nyquist plot of $F(s)H(s)$,in Figure 6, show no encirclements to the point (-1,0) with phase and gain margins of $P_M\to\infty$ and $G_M=14dB's$, respectively; hence, polynomial $B(s)$ is stable and robust and, consequently, the NR-DOB control system is also stable and robust.

Finally, time responses of $T_R(s)R(s)$, $S_d(s)d(s)$, $S_\delta(s)\delta(s)$ and $S_\eta(s)\eta(s)$, with $R(s)=d(s)=\delta(s)=\eta(s)$ all assumed unity step signals are shown in Figure 7.

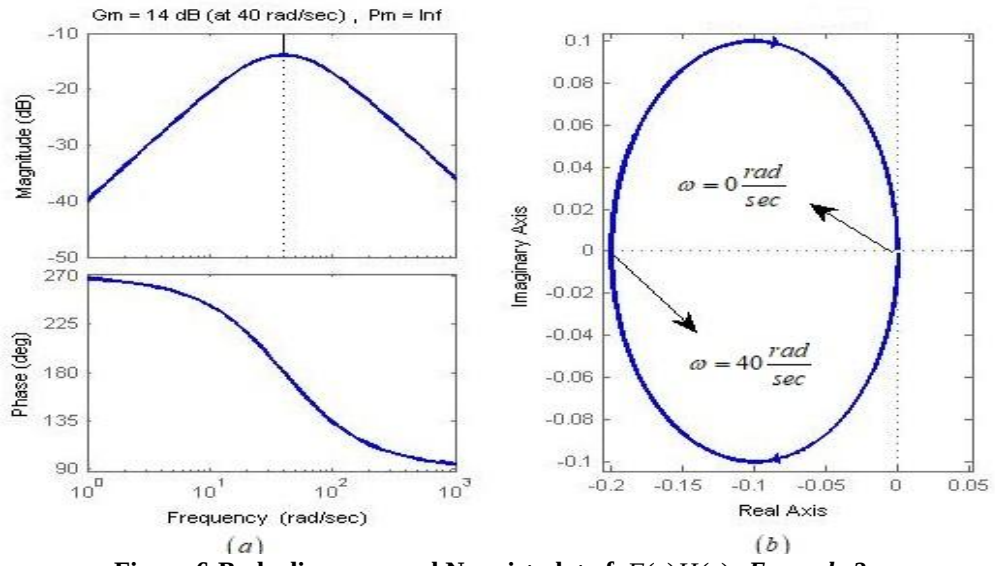

Figure 6:Bode diagrams and Nyquist plot of $F(s)H(s)$**.** ***Example 2***

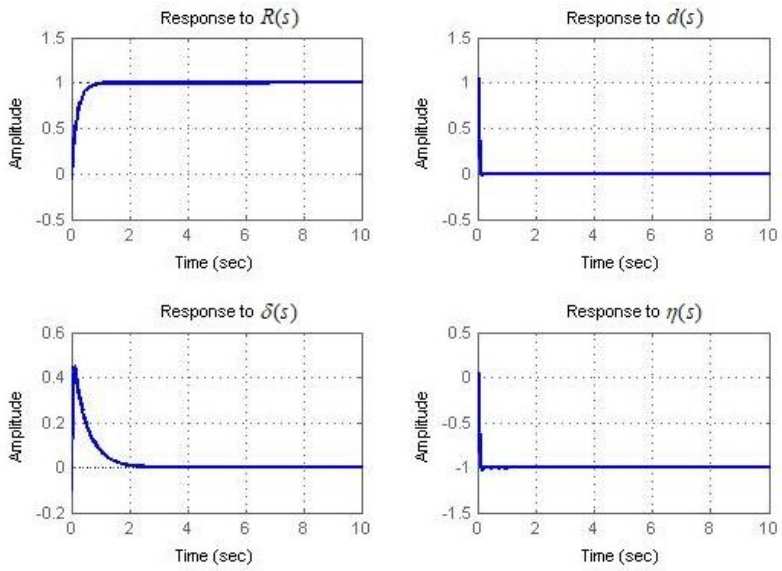

Figure 7: $T_R(s), S_d(s), S_\delta(s)$ **and** $S_\eta(s)$ **step responses.** ***Example 2***

To assess the robustness properties the plant is modified as $G(s) = 0.125\dfrac{-s+80}{(s+2)(0.1s+1)}$; that is, assuming a variation of 20% in the non-minimum phase zero and an additional non-modelled pole at *-10*. The step responses shown in Figure 8 prove that the designed NR-DOB control system can maintain stability and performance despite process uncertainties, proving its robustness.

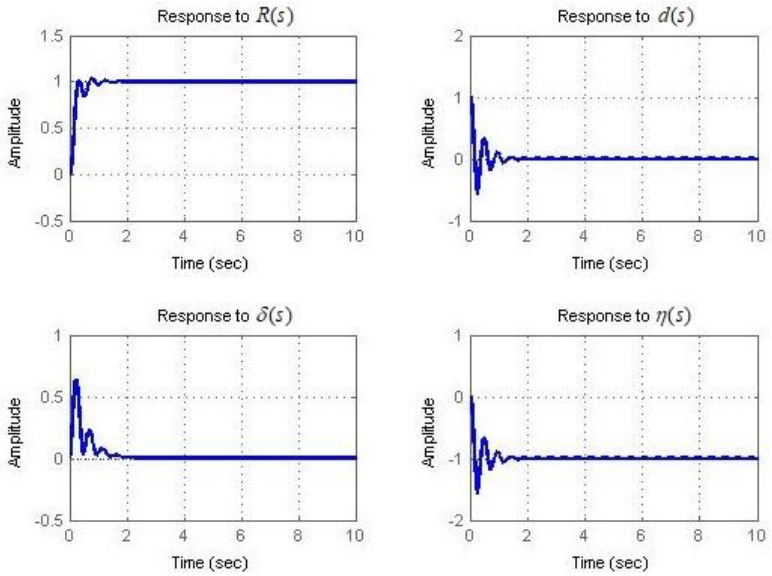

Figure 8: $T_R(s), S_d(s), S_\delta(s)$ **and** $S_\eta(s)$ **step responses with modified plant.** ***Example 2***

It is important to notice from *Example 2* that process $G(s)$ can be non-minimum phase, contrary to the conditions reported in [9].

- *Unstable process*

Example 3: Let the unstable process $G(s)=\frac{4}{-s^2-s+2}$. To propose an unstable model $\tilde{G}(s)$, trying to match the process, will result in $\tilde{G}(s)^{-1}G(s)$ with an exact or almost exact unstable cancellations leading to the non-existence of a filter $F(s)$ capable of stabilizing polynomial $B(s)$ as required by condition *ii* of *Lemma 1*.
Therefore, and based on condition *ii* of *Lemma 1*, to assure the appropriate number of anti-clock sense encirclements to the point (-1,0) by the Nyquist plot of $H(s)$ and existence of a stabilizer filter $F(s)$, model $\tilde{G}(s)$ should be assumed stable with negative gain such that $\tilde{G}(s)^{-1}G(s)$ is minimum phase with a Nyquist plot located in $\square_2^-$ rotating counter clockwise. Additionally, $\left|\tilde{G}(j\omega)\right|<\left|G(j\omega)\right|$ to assure sufficient high gain so the unstable pole of $\tilde{G}(s)^{-1}G(s)$ can be stabilized.
A suitable model $\tilde{G}(s)$ complying with these conditions is given by:

$$\tilde{G}(s)=-\frac{1}{s^2+3s+2} \tag{11}$$

Similar to the two previous examples the first step, according to condition *i*of *Lemmas 1*and *2*, is to design a stabilizing controller $C(s)$ for model $\tilde{G}(s)$ with adequate robustness margins. A controller complying with these requirements is given by:

$$C(s)=-1.8\frac{(0.5s+1)}{s} \tag{12}$$

Bode plot of $C(s)\tilde{G}(s)$, in Figure 9, shows that condition *i*of *Lemmas 1* and *2* are satisfied with phase and gain margins of $P_M=54^o$ and $G_M\to\infty$, respectively.

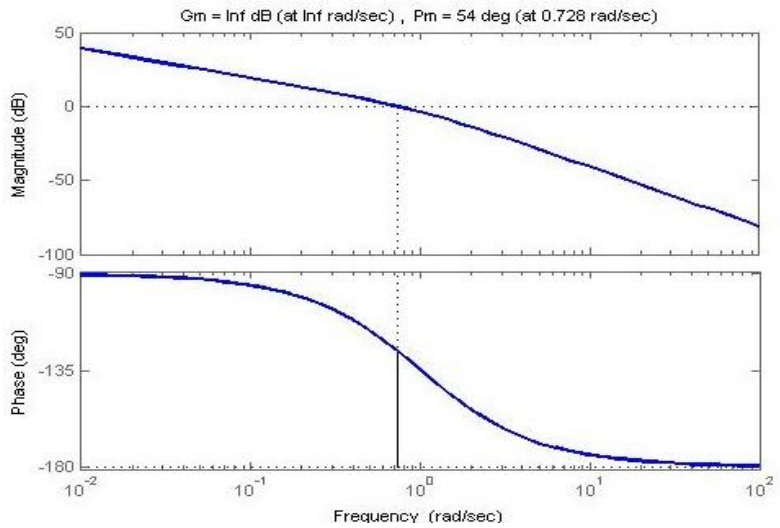

Figure 9:Bode Diagrams and robustness margins of $C(s)\tilde{G}(s)$. *Example 3*

The design of filter $F(s)$ requires to calculate $\tilde{G}(s)^{-1}G(s)$, resulting in:

$$\tilde{G}(s)^{-1}G(s)=4\frac{(s+1)}{(s-1)} \tag{13}$$

Because $\tilde{G}(s)^{-1}G(s)$ Nyquist plot encircles point (1,0) once in counter clockwise, Figure 10, $H(s)$ will be minimum phase; in fact, $H(s)$ results in:

$$H(s) = -\left(1 - \frac{G(s)}{\tilde{G}(s)}\right) = -\frac{(3s+5)}{(s-1)} \tag{14}$$

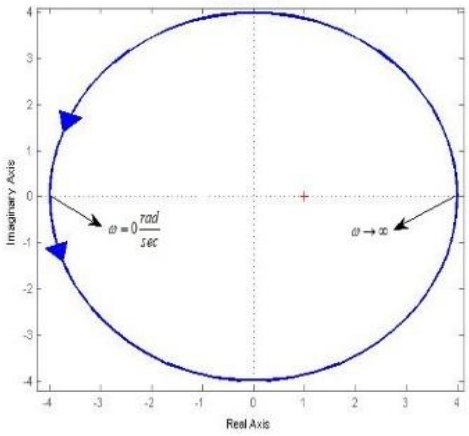

Figure 10:Nyquist plot of $C(s)\tilde{G}(s)^{-1}$. *Example 3*

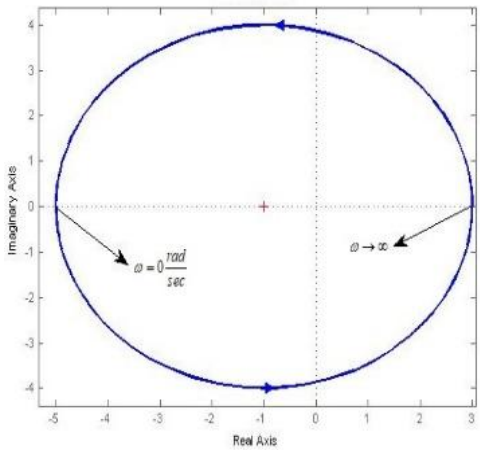

Figure 11:Nyquist plot of $H(s)$. *Example 3*

The Nyquist plot of $H(s)$, Figure 11, shows one anti-clockwise encirclement to point (-1,0). Hence, filter $F(s)$ must be designed with sufficient high bandwidth ω_{B_F} such that the anti-clock wise encirclement to the point (1,0) is maintained by $F(s)H(s)$. This must be done with adequate robust margins and assuring $F(s)\tilde{G}(s)^{-1}$ causal. An appropriate filter $F(s)$ is given by:

$$F(s) = \frac{1}{(0.05s+1)^2} \tag{15}$$

Resulting in a stable and robust polynomial $B(s)$ as shown in Figure 12 where theBode diagrams of $F(s)H(s)$ show robust margins of $P_M = 65.1^o$ and $G_M \to -14dB's$, respectively, and the $F(s)H(s)$ Nyquist plot keeps the anti-clockwise encirclement to the point (-1,0). Therefore, condition *ii* of *Lemmas 1* and *2* are satisfied.

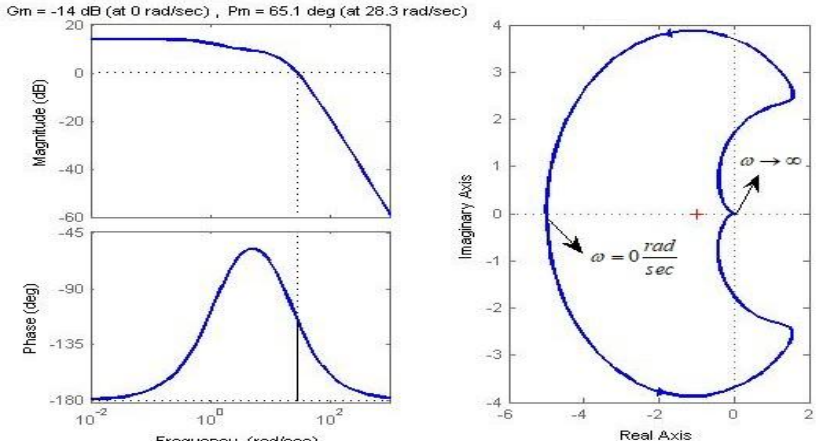

Figure 12:Bode Diagrams and Nyquist plot of $F(s)H(s)$ **.** ***Example 3***

Time responses of $T_R(s)R(s)$, $S_d(s)d(s)$, $S_\delta(s)\delta(s)$ and $S_\eta(s)\eta(s)$, with $R(s)=d(s)=\delta(s)=\eta(s)$ all assumed unity step signals are shown in Figure 13.

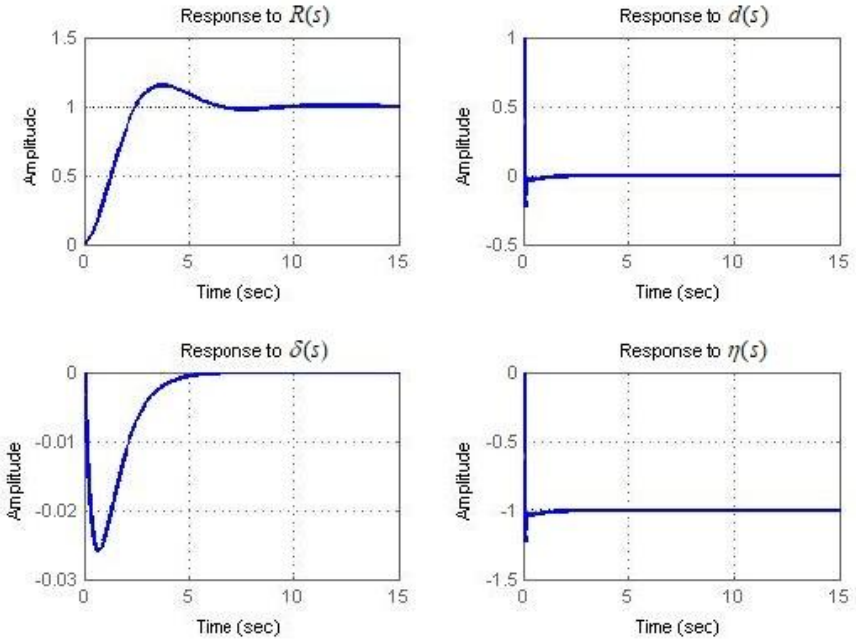

Figure 13: $T_R(s), S_d(s), S_\delta(s)$ **and** $S_\eta(s)$ **step responses.** ***Example 3***

Similar to example 2 the plant is modified as $G(s)=\dfrac{2}{\left(-s^2-s+2\right)\left(0.1s+1\right)}$; that is, with a variation of 50% in the gain and a neglected stable pole at -10. The step responses with the modified plant, in Figure 14, prove the robustness properties of the design.

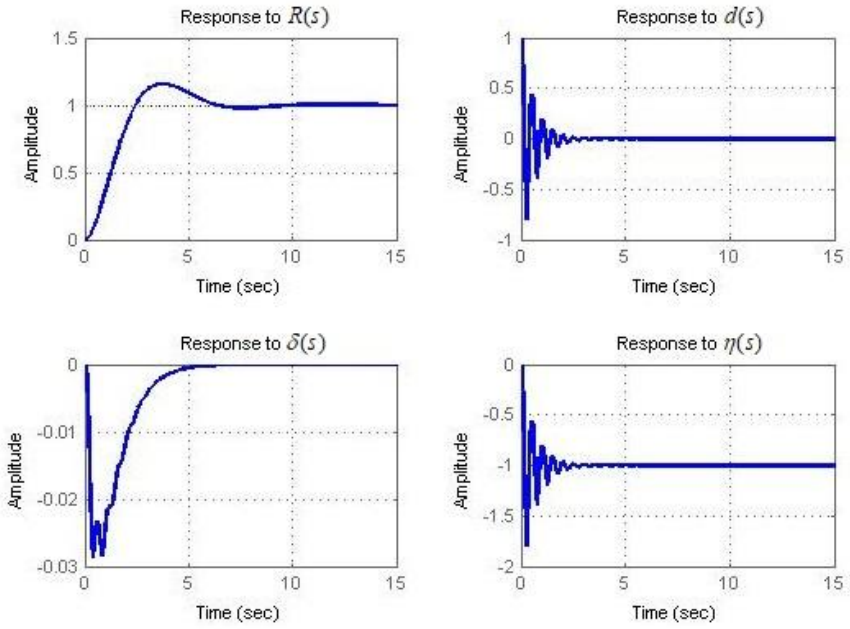

Figure 14: $T_R(s), S_d(s), S_\delta(s)$ **and** $S_\eta(s)$ **step responses with modified plant.** ***Example 3***

Thanks to the transparency of classical control theory, *Example 3* proves that it is possible to apply the NR-DOB to unstable processes assuring performance and robustness. However, and contrary to normal procedures, it is also proven that process model must not be designing trying to match the process. Instead, its design should aim to achieve stability. Further analysis indicates that $\tilde{G}(s)$ over-parametrized with stable poles is recommended since this will generate a non-causal minimum phase $\tilde{G}(s)^{-1}G(s)$ which in turn will induce sufficient anticlockwise encirclements to point (-1,0) by $H(s)$ so $[1+H(s)]=0$ will be stable; remaining only the design of filter $F(s)$ with sufficient bandwidth ω_{B_F} and degree n.

- *Process with time delay*

Example 4: Let a stable minimum phase process with a time delay d, $G(s)=e^{-ds}k\dfrac{s^m+b_{m-1}s^{m-1}+...+b_1s+b_0}{s^n+a_{n-1}s^{s-1}+...+a_1s+a_0}$ with $m\le n$. Because $F(s)\tilde{G}(s)^{-1}$ must be causal, $\tilde{G}(s)$ cannot be designed trying to match process $G(s)$ time delay; otherwise, there will not be a filter $F(s)$ capable of guaranteeing causality in $F(s)\tilde{G}(s)^{-1}$, given that an $F(s)$ of infinite degree will be required.

On the other hand, assume model $\tilde{G}(s)$ stable and minimum phase in the form of $\tilde{G}(s)=\tilde{k}\dfrac{s^{\tilde{m}}+\tilde{b}_{\tilde{m}-1}s^{\tilde{m}-1}+...+\tilde{b}_1s+\tilde{b}_0}{s^{\tilde{n}}+\tilde{a}_{\tilde{n}-1}s^{s-1}+...+\tilde{a}_1s+\tilde{a}_0}$ with $\tilde{m}\le\tilde{n}$. If $\tilde{n}<n$, $\tilde{G}(s)^{-1}G(s)$ will be causal with relative degree $\text{Re\_deg}\left(\tilde{G}(s)^{-1}G(s)\right)=n\tilde{m}-\tilde{n}m>0$, such that $\lim_{\omega\to\infty}\tilde{G}(s)^{-1}G(s)=0$, rendering a $\tilde{G}(s)^{-1}G(s)$ Nyquist plot with magnitude tending to zero with infinite clockwise encirclements to the origin due to $G(s)$ time delay. This will induce infinite clockwise encirclements to point (-1,0) by $H(j\omega)$, so polynomial $B(s)=[1+F(s)H(s)]$ will be unstable unless filter $F(s)$ bandwidth ω_{B_F} is chosen sufficiently small to avoid $F(j\omega)H(j\omega)$ clockwise encirclements to (-1,0).

In the case of $n<\tilde{n}$, $\tilde{G}(s)^{-1}G(s)$ will be non-causal with relative degree $\text{Re\_deg}\left(\tilde{G}(s)^{-1}G(s)\right)=n\tilde{m}-\tilde{n}m<0$

and $\lim_{\omega\to\infty}\tilde{G}(s)^{-1}G(s)\to\infty$ which, similar to the previous case, due to process $G(s)$ time delay will induce infinite clockwise encirclements to the origin with magnitude tending to infinite, which in turn will induce infinite clockwise encirclements to point (-1,0) by $H(j\omega)$. Therefore, polynomial $B(s)=\left[1+F(s)H(s)\right]$ will be stable provided filter $F(s)$ not only with sufficiently small bandwidth ω_{B_F} but with a degree $\deg(F(s))>|n\tilde{m}-\tilde{n}m|$ to generate sufficient roll-off in $F(s)H(s)$ so high frequency clockwise encirclements to (-1,0) are avoided.

Something similar occurs when $\text{Re\_deg}\left(\tilde{G}(s)^{-1}G(s)\right)=n\tilde{m}-\tilde{n}m=0$, as this will induce infinite clockwiseencirclements to point (-1,0) with constant magnitude $\left|k/\tilde{k}\right|$ by $H(j\omega)$ which will require, as the two previous cases, filter $F(s)$ bandwidth ω_{B_F} sufficiently small to avoid $F(j\omega)H(j\omega)$ clockwise encirclements to point (1,0).

Based on the previous analysis, consider a process given by $G(s)=e^{-0.05s}\dfrac{1}{(s+2)^2}$ and a process model $\tilde{G}(s)=\dfrac{1}{(s+1.5)(s+2.5)}$ such that $\tilde{G}(s)^{-1}G(s)=e^{-0.05s}\dfrac{(s+1.5)(s+2.5)}{(s+2)^2}$ with relative degree $\text{Re\_deg}\left(\tilde{G}(s)^{-1}G(s)\right)=n\tilde{m}-\tilde{n}m=0$. The Nyquist plot of $\tilde{G}(s)^{-1}G(s)$, Figure 15.a, shows the infinite clockwise encirclements with magnitude $\left|k/\tilde{k}\right|=1$ to the origin, inducing infinite clockwise encirclements to point (-1,0) by $H(j\omega)$ as shown in Figure 15.b.

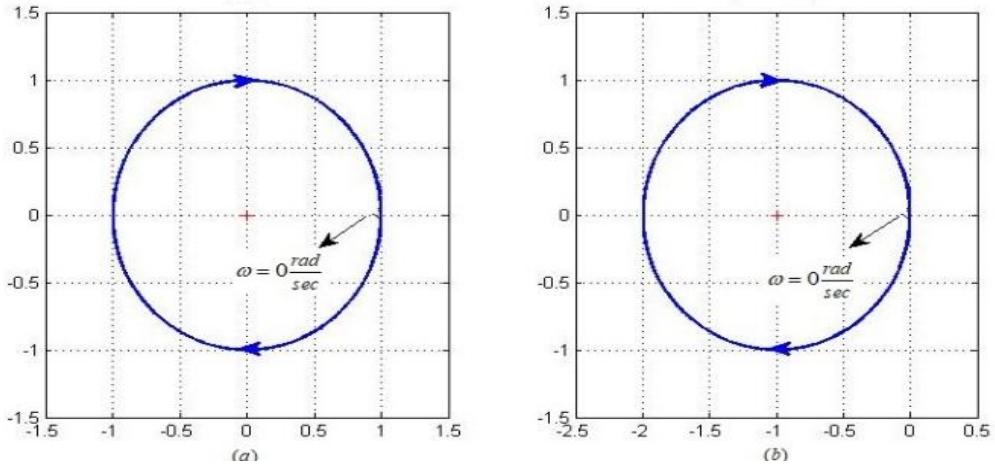

Figure 15Nyquist plots of $\tilde{G}(s)^{-1}G(s)$ and $H(s)$. *Example 4*

To avoid the clockwise encirclements to (-1,0) $F(s)$ bandwidth ω_{B_F} must be chosen sufficiently small with a degree such that $F(s)\tilde{G}(s)^{-1}$ is causal resulting in:

$$F(s)=\frac{1}{(0.09s+1)^3} \tag{16}$$

The resulting Bode diagrams and Nyquist plot of $F(s)H(s)$ are shown in Figure 16, where it is shown that the clockwise encirclements to point (-1,0) are avoided with phase and gain margins of $P_M\to\infty$ and $G_M=14.01dB's$, respectively. Therefore, polynomial $B(s)$ is stable and robust according to condition *ii* of *Lemmas 1* and *2*.

To comply with conditions *i*of *Lemmas 1* and *2*, is necessary to design a stabilizer controller $C(s)$ for model $\tilde{G}(s)$ with appropriate robust margins. A suitable PI controller is given by:

$$C(s) = 2.7\frac{(s+1.5)}{s} \tag{17}$$

In Figure 17 the Bode diagrams of $C(s)\tilde{G}(s)$ shows adequate robust margins of $P_M = 68.2^o$ and $G_M \to \infty dB's$. Hence, polynomial $A(s)$ is stable and robust.

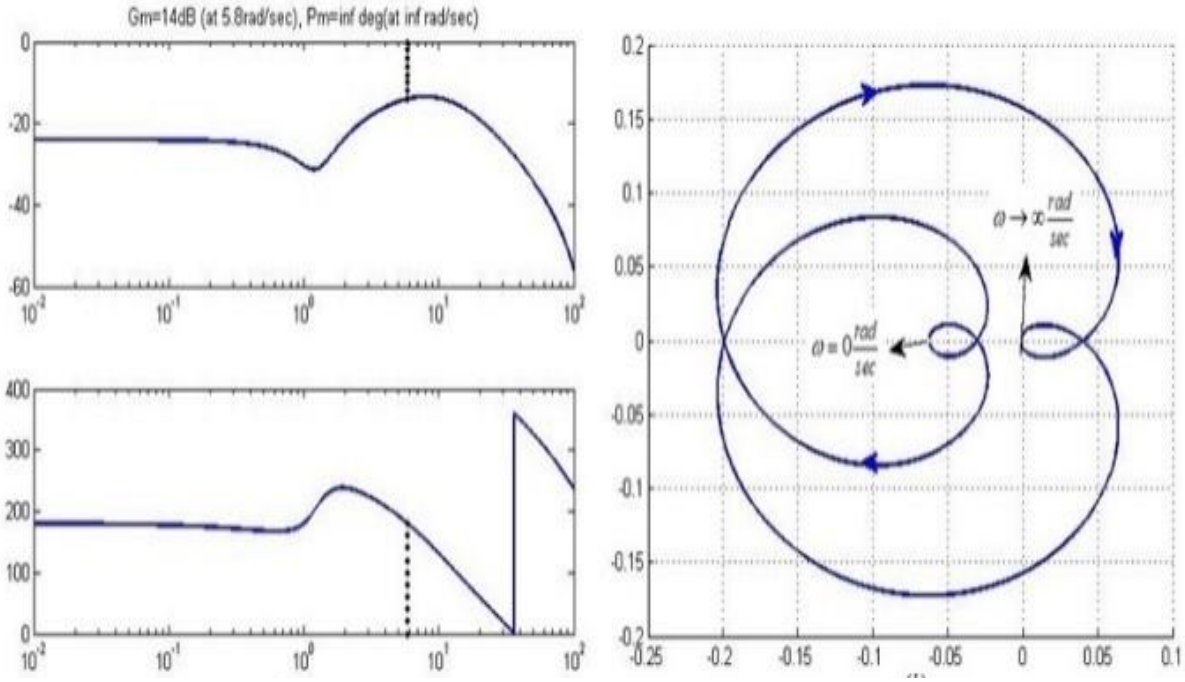

Figure 16:Bode Diagrams and Nyquist plot of $F(s)H(s)$ **.** ***Example 4***

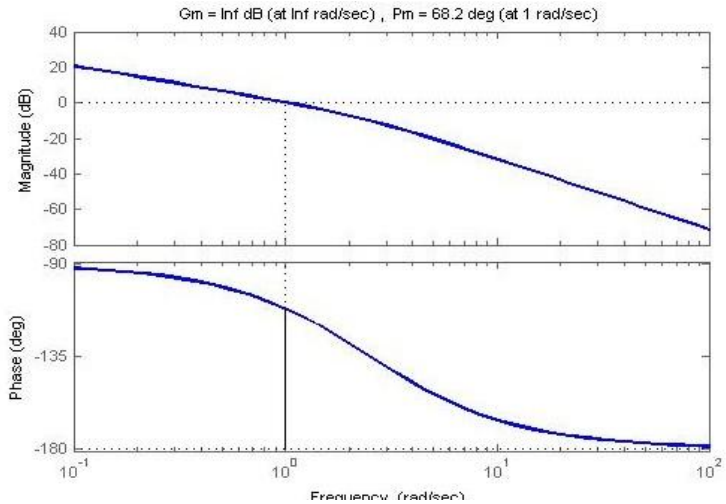

Figure 17:Bode Diagrams and robust margins of $C(s)\tilde{G}(s)$ **.** ***Example 4***

Finally, time responses of $T_R(s)R(s)$, $S_d(s)d(s)$, $S_\delta(s)\delta(s)$ and $S_\eta(s)\eta(s)$, with $R(s) = d(s) = \delta(s) = \eta(s)$ all assumed unity step signals are shown in Figure 18.

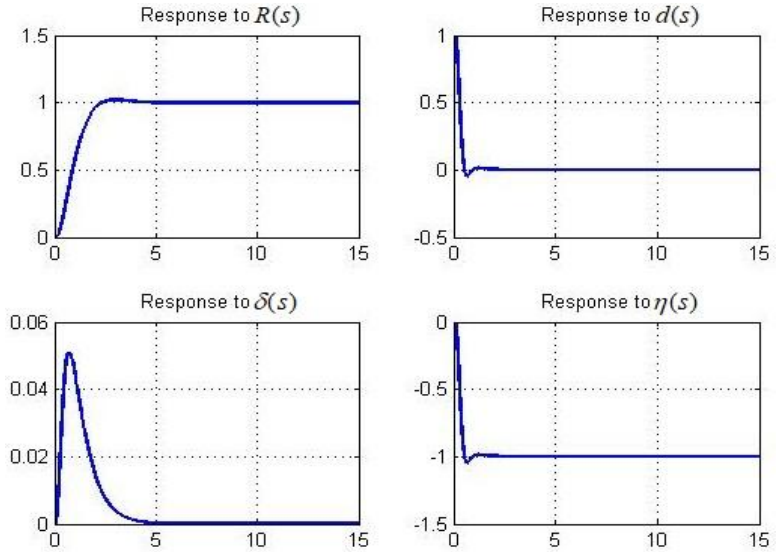

Figure 18: $T_R(s), S_d(s), S_\delta(s)$ **and** $S_\eta(s)$ **step responses.** ***Example 4***

Similar to previous examples the plant is modified as $G(s) = e^{-0.1s}\dfrac{1}{(s+2)^2(0.1s+1)}$; that is, with a time delay increment of 100% and a neglected stable pole at -10. The step responses with the modified plant, in Figure 19, prove the robustness properties of the design.

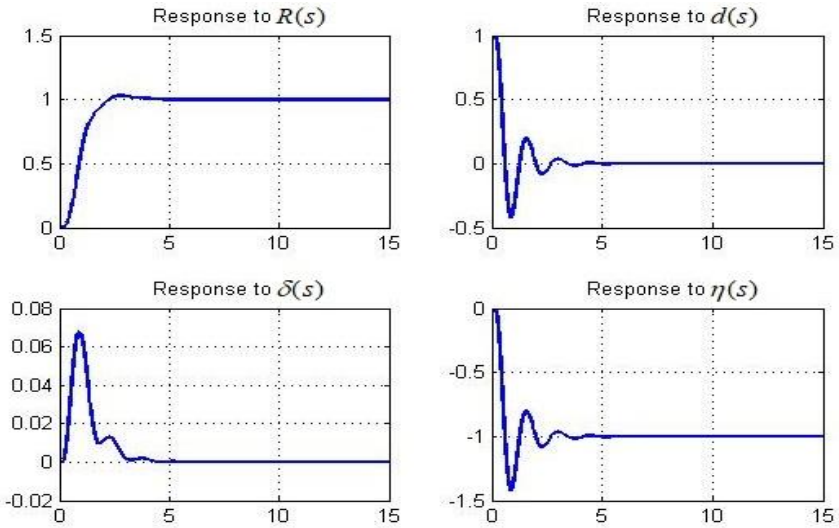

Figure 19: $T_R(s), S_d(s), S_\delta(s)$ **and** $S_\eta(s)$ **step responses with modified plant.** ***Example 4***

V. CONCLUSION

Based on the Nyquist stability criteria, global stability, and robustness conditions for linear Noise Reduction Disturbance Observer (NR-DOB) control systems are established. The approach here presented, thanks to its classical control nature, allows a transparent analysis and design in the frequency domain of NR-DOB control systems assuring stability, robustness, and performance. Also, based on the conditions here presented, through several examples it was proved that contrary to previous reports, it is possible to design NR-DOB control systems for unstable and non-minimum phase processes, including time delay. However, to achieve this, it was also found that process model should be designed with stability purposes rather than process matching. This is particularly critical in the case of unstable process or process including time delay. Hence, a control system based on the NR-DOB is in general a 3 DOF rather than a 2 DOF control strategy.

REFERENCES

[1]. Wei Xie, "High frequency measurement noise rejection based on disturbance observer". Journal of the Franklin Institute 347, pp.1825–1836, 2010.

[2]. Wen-Hua Chen. "Disturbance Observer Based Control for Nonlinear Systems". IEEE/ASME Transactions on Mechatronics, 9 (4), pp. 706-710 [10.1109/TMECH.2004.839034], 2006.

[3]. VaijayantiS.Deshpande, B.Mohan, P.D.Shendge and S.B.Phadke. "Disturbance observer-based sliding mode control of active suspension systems". Journal of Sound and Vibration, Vol. 333, pp. 2281–2296Z. 2014.

[4]. Jun Yang, Shihua Li ∗, Xisong Chen, Qi Li. "Disturbance rejection of dead-time processes using disturbance observer and model predictive control". Chemical Engineering Research and Design, Vol. 89, pp. 125–135. 2011.

[5]. Sujay D. Kadam1 and L. M. Waghmare. "Control of Integrating Processes with Dead-Time using PID Controllers with Disturbance Observer based Smith Predictor". 2013 IEEE International Conference on Control Applications (CCA) Part of 2013 IEEE Multi-Conference on Systems and Control. 2013.

[6]. X.S. Chen, J. Yang, S.H. Li and Q. Li. "Disturbance observer based multi-variable control of ball mill grinding circuits". Journal of Process Control, Vol 19, pp. 1205–1213, 2009.

[7]. Noriaki Hirose, Ryosuke Tajima, Nagisa Koyama, KazutoshiSukigara and Minoru Tanaka. "Following control approach based on model predictive control for wheeled inverted pendulum robot". Advanced Robotics 30:6, pages 374-385. 2016.

[8]. H. Shim and Y. Joo. "State Space Analysis of Disturbance Observer and Robust Stability Condition". In Proc. Of 46th IEEE conference on Decision and Control, 2007.

[9]. Nam H. Jo and Hyungbo Shim. "Robust Stabilization via Disturbance Observer with Noise Reduction". European Control Conference (ECC) Zürich, Switzerland. 2013.

[10]. Hyungbo SHIM, Gyunghoon PARK, Youngjun JOO, Juhoon BACK, Nam Hoon JO. "Yet Another Tutorial of Disturbance Observer: Robust Stabilization and Recovery of Nominal Performance Control". Theory Tech, Vol.14, No.3, pp.237–249, August 2016 Control Theory and Technology, http://link.springer.com/journal/11768

[11]. Emre SARIYILDIZ, Kouhei OHNISHI. "On the Robustness of Disturbance Observer". AMC2014-Yokohama, March 14-16, 2014, Yokohama, Japan

[12]. Emre Sariyildiz and Kouhei Ohnishi. "Stability and Robustness of Disturbance-Observer-Based Motion Control Systems". IEEE TRANSACTIONS ON INDUSTRIAL ELECTRONICS, VOL. 62, NO. 1, JANUARY 2015.

[13]. Sehoon Oh, Hanseung Woo and Kyoungchul Kong. "Stability and Robustness Analysis of Frequency-shaped Impedance Control for Reference Tracking and Compliant Interaction". Preprints of the 19th World Congress the International Federation of Automatic Control Cape Town, South Africa. August 24-29, 2014.

[14]. Jong Nam Yun and Jian-Bo Su, (2014). "Design of a Disturbance Observer for a Two-Link Manipulator with Flexible Joints". IEEE TRANSACTIONS ON CONTROL SYSTEMS TECHNOLOGY, Vol. 22, No. 2, march 2014.

[15]. Emre Sariyildiz&Kouhei Ohnishi. "Analysis the robustness of control systems based on disturbance observer". International Journal of Control, Vol.86 – Issue 10, pp. 1733-1743 citation https://doi.org/10.1080/00207179.2013.795663, 2013.